

The hexosamine biosynthesis pathway and O-GlcNAcylation maintain insulin-stimulated PI3K-PKB phosphorylation and tumour cell growth after short-term glucose deprivation

David R. Jones¹, Willem-Jan Keune¹, Karen E. Anderson², Len R. Stephens², Phillip T. Hawkins² and Nullin Divecha^{1,3}

¹ Inositide Laboratory, Cancer Research UK Manchester Institute, University of Manchester, UK

² The Babraham Institute, Cambridge, UK

³ Inositide laboratory, Centre for Biological Sciences, University of Southampton, Southampton, UK

Keywords

glucose; insulin; oxidative stress; protein kinase B; Signalling

Correspondence

N. Divecha, Inositide Laboratory, Centre for Biological Sciences, University of Southampton, Southampton UK.
E-mail: N.divecha@soton.ac.uk

(Received 18 February 2014, revised 9 May 2014, accepted 12 June 2014)

doi:10.1111/febs.12879

Glucose provides an essential nutrient source that supports glycolysis and the hexosamine biosynthesis pathway (HBP) to maintain tumour cell growth and survival. Here we investigated if short-term glucose deprivation specifically modulates the phosphatidylinositol 3-kinase/protein kinase B (PI3K/PKB) cell survival pathway. Insulin-stimulated PKB activation was strongly abrogated in the absence of extracellular glucose as a consequence of the loss of insulin-stimulated PI3K activation and short-term glucose deprivation inhibited subsequent tumour cell growth. Loss of insulin-stimulated PKB signalling and cell growth was rescued by extracellular glucosamine and increased flux through the HBP. Disruption of *O*-GlcNAc transferase activity, a terminal step in the HBP, implicated *O*-GlcNAcylation in PKB signalling and cell growth. Glycogenolysis is known to support cell survival during glucose deprivation, and in A549 lung cancer cells its inhibition attenuates PKB activation which is rescued by increased flux through the HBP. Our studies show that rerouting of glycolytic metabolites to the HBP under glucose-restricted conditions maintains PI3K/PKB signalling enabling cell survival and proliferation.

Introduction

The continuous requirement for both extracellular carbon and nitrogen energy supply dictates that cells must be able to adapt to abrupt changes in their local environment in order to maintain adequate flux through metabolic pathways. Cells have evolved pathways that couple changes in nutrient supply to the regulation of critical pathways such as cell growth, protein synthesis, DNA replication and gene transcription [1]. For exam-

ple the LKB1/AMPK/MTORC1 pathway forms a critical axis that couples nutrient sensing to the regulation of metabolic activity, mRNA translation, cell growth, cell proliferation and cell differentiation [2–6]. In response to glucose deprivation the activation of AMPK by LKB1 functions to attenuate anabolic pathways such as the mammalian target of rapamycin complex 1 (mTORC1) pathway and inhibit cell growth as

Abbreviations

GSH, glutathione; HBP, hexosamine biosynthesis pathway; IGF1, insulin-like growth factor 1; IRS-1, insulin receptor substrate 1; mTORC1, mammalian target of rapamycin complex 1; OGA, *O*-GlcNAcylase; OGT, *O*-GlcNAc transferase; PDK1, phosphoinositide-dependent protein kinase 1; PI3K, phosphatidylinositol 3-kinase; PKB, protein kinase B; PPP, pentose phosphate pathway; PtdIns(3,4)P₂, phosphatidylinositol (3,4)-bisphosphate; PtdIns(3,4,5)P₃, phosphatidylinositol(3,4,5)-trisphosphate; shRNA, small hairpin RNA; UDP-GlcNAc, uridine diphosphate *N*-acetylglucosamine.

well as rewiring metabolic pathways aimed at preventing catastrophic low energy stress-induced apoptosis. Other key intracellular metabolites are also monitored in order to couple nutrient supply to cellular pathways and include glutamine, NAD^+ and acetyl-CoA [7,8].

In mammals, cells and tissues normally encounter a constant supply of nutrients; however, during tumour development gradients of nutrients such as glucose, lipids and oxygen occur as a consequence of poor vascularization [9]. This hypoxic and nutrient-restricted tumour microenvironment not only selects for cells which have deregulated crosstalk between nutrient sensing pathways and the regulation of cell growth but also can induce genetic and epigenetic changes that enable the expansion and metastasis of the most aggressive malignant tumour cells [10–12]. These adaptive measures include upregulation of transporters to increase glucose and amino acid uptake and in fact increased glucose uptake is often used to define tumours by positron emission tomography [13,14]. Increased glucose uptake fuels glycolysis and even in the presence of oxygen tumour cells often convert pyruvate to lactate, to replenish reducing equivalents, rather than utilizing the tricarboxylic acid cycle [15–17]. This energetically inefficient use of glucose is thought to support the requirement for glycolytic intermediates. Intracellular glucose is a critical nutrient, which supports three important pathways. It can be converted to glucose 1-phosphate by phosphoglucomutase for glycogen synthesis, converted to fructose 6-phosphate by phosphoglucose isomerase for glycolysis or converted to 6-phosphoglucono- δ -lactone by glucose 6-phosphate dehydrogenase for entry into the pentose phosphate pathway (PPP). Flux through the PPP provides substrates for RNA and DNA synthesis as well as increasing the reducing potential of the cells [18].

In addition, flux through the hexosamine biosynthesis pathway (HBP) is also dependent on glucose supply [19]. Metabolites from glycolysis enter the HBP by the conversion of fructose 6-phosphate to glucosamine 6-phosphate by glutamine fructose-6-phosphate amidotransferase which is the rate limiting entry step of the HBP. Flux through the HBP integrates carbohydrate, fat, protein and nucleotide metabolism, with the generation of uridine diphosphate *N*-acetylglucosamine (UDP-GlcNAc) [20]. UDP-GlcNAc is required for the synthesis of glycolipids, glycosaminoglycans and glycoproteins [21,22]. As many growth factor receptors including the insulin and insulin-like growth factor 1 (IGF1) receptor are N-glycosylated, flux through the HBP couples nutrient availability to receptor activation. Furthermore growth factor receptor activation also impacts on intracellular nutrient supply by regulating nutrient uptake [23].

UDP-GlcNAc is also the sugar donor for protein *O*-GlcNAcylation. *O*-GlcNAcylation of specific serine and threonine residues is catalysed by *O*-GlcNAc transferase (OGT) and reversed by the action of *O*-GlcNAcylase (OGA) to enable dynamic post-translational modification of proteins which can regulate protein localization, stability, aggregation and interaction with other proteins. Protein *O*-GlcNAcylation impacts directly on cell processes including metabolism and gene transcription [24].

Thus utilization of glucose not only provides energy for the cell, but also enables the diversion of glycolytic intermediates into the PPP and HBP to provide the building blocks to drive cell growth, division and proliferation and link major metabolic pathways with protein *O*-GlcNAcylation signalling. Increased flux through the PPP and the HBP are required for development of some tumours and in part might explain the enhanced uptake of glucose by tumour cells [10,25–27].

Insulin/IGF1 receptors are important in both normal and tumour physiology [28–30]. They drive metabolic and proliferative responses through ligand-mediated activation of their intrinsic tyrosine kinase activity. Tyrosine phosphorylation of the receptor itself and of adaptor proteins such as insulin receptor substrate 1 (IRS-1) induce the recruitment of phosphatidylinositol 3-kinase (PI3K) which stimulates phosphatidylinositol(3,4,5)-trisphosphate [PtdIns(3,4,5) P_3] synthesis [31–33]. This leads to the activation of numerous downstream proteins including protein kinase B (PKB), which impact cell proliferation, cell survival and metabolic processes. While activation of the mTORC1 pathway downstream of the insulin receptor has been shown to be sensitive to glucose levels, much less is understood about glucose-dependent regulation of the insulin/PI3K/PKB pathway.

Herein we have investigated whether activation of the PI3K/PKB pathway is sensitive to extracellular glucose. We found that short-term glucose deprivation severely restricts insulin-stimulated PKB activation and long-term U2OS tumour cell growth, both of which could be rescued by extracellular glucosamine and increased flux through the HBP and *O*-GlcNAcylation. Glucose deprivation attenuates insulin-induced IRS-1 phosphorylation, PI3K recruitment and PtdIns(3,4,5) P_3 synthesis all of which are rescued by extracellular glucosamine. The data suggest that, under restricted glucose availability, the HBP and *O*-GlcNAcylation permit insulin-induced PKB signalling to enable long-term responses such as cell proliferation.

Results

Exogenously added glucosamine rescues PKB activation by insulin and oxidative stress during energy restriction

In order to study pathways that might be sensitive to glucose we deprived U2OS cells of glucose for 6 h and then replenished the medium and monitored cell growth. Surprisingly, short-term glucose deprivation completely suppressed cell growth over the following 7 days (Fig. 1A). U2OS cell growth requires the PI3K/mTOR/PKB pathway [34] and therefore we assessed PKB activation in response to oxidative stress or insulin stimulation after 6 h of glucose deprivation, conditions under which the cells appeared morphologically normal, with minimal evidence of cell death (Fig. 1B).

Oxidative stress [hydrogen peroxide (H_2O_2)] and insulin increased phosphorylation of PKB at residues Ser473 and Thr308 when cells were maintained in glucose but not in cells deprived of glucose (Fig. 1C,D). Glucose deprivation strongly attenuated protein O-GlcNAcylation (Fig. 1C) showing that HBP flux in U2OS cells was dependent on extracellular glucose supply (substrate driven). In order to test whether the HBP might influence the activation of PKB by both insulin and H_2O_2 we added extracellular glucosamine to cells maintained in the absence of glucose. Glucosamine directly enters the HBP (Fig. 2A) and accordingly we found that extracellular glucosamine increased protein O-GlcNAcylation in glucose-deprived cells (Fig. 2B). The specificity of the antibody used to detect protein O-GlcNAcylation was demonstrated by

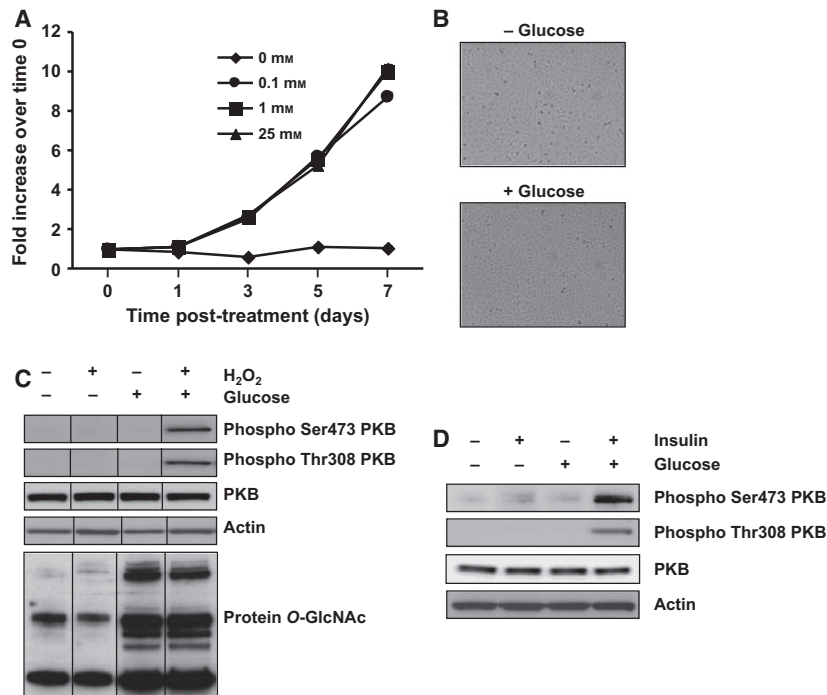


Fig. 1. (A) U2OS cells were plated at low density (30 000 per well) in six-well plates using complete medium. The next day the cells were washed four times with $NaCl/P_i$ before maintaining them for 6 h in serum- and glucose-free DMEM supplemented with different concentrations of glucose followed by media removal and replacement with serum- and glucose-containing DMEM. At intervals thereafter, cell monolayers were washed twice with $NaCl/P_i$ before staining with crystal violet. Crystal violet stain was solubilized and quantitated by spectrophotometry. The graph represents mean \pm SD ($n = 3$). (B) U2OS cells were plated in six-well plates using complete medium. The next day the cells were washed four times with $NaCl/P_i$ before maintaining them for 6 h in serum- and glucose-free DMEM supplemented as indicated. Photographs were taken using a camera fitted to a microscope. (C) U2OS cells were plated in six-well plates using complete medium. The next day the cells were washed four times with $NaCl/P_i$ before maintaining them for 6 h in serum- and glucose-free DMEM supplemented as indicated. The cells were control-treated or treated with 1 mM H_2O_2 for 15 min. Thereafter, cell lysates were prepared and western blotting was performed using the indicated antibodies. (D) U2OS cells were plated in six-well plates using complete medium. The next day the cells were washed four times with $NaCl/P_i$ before maintaining them for 6 h in serum- and glucose-free DMEM supplemented as indicated. The cells were control-treated or treated with 1 $\mu g \cdot mL^{-1}$ insulin for 15 min. Thereafter cell lysates were prepared and western blotting was performed using the indicated antibodies. Representative photographic images and western blots are shown.

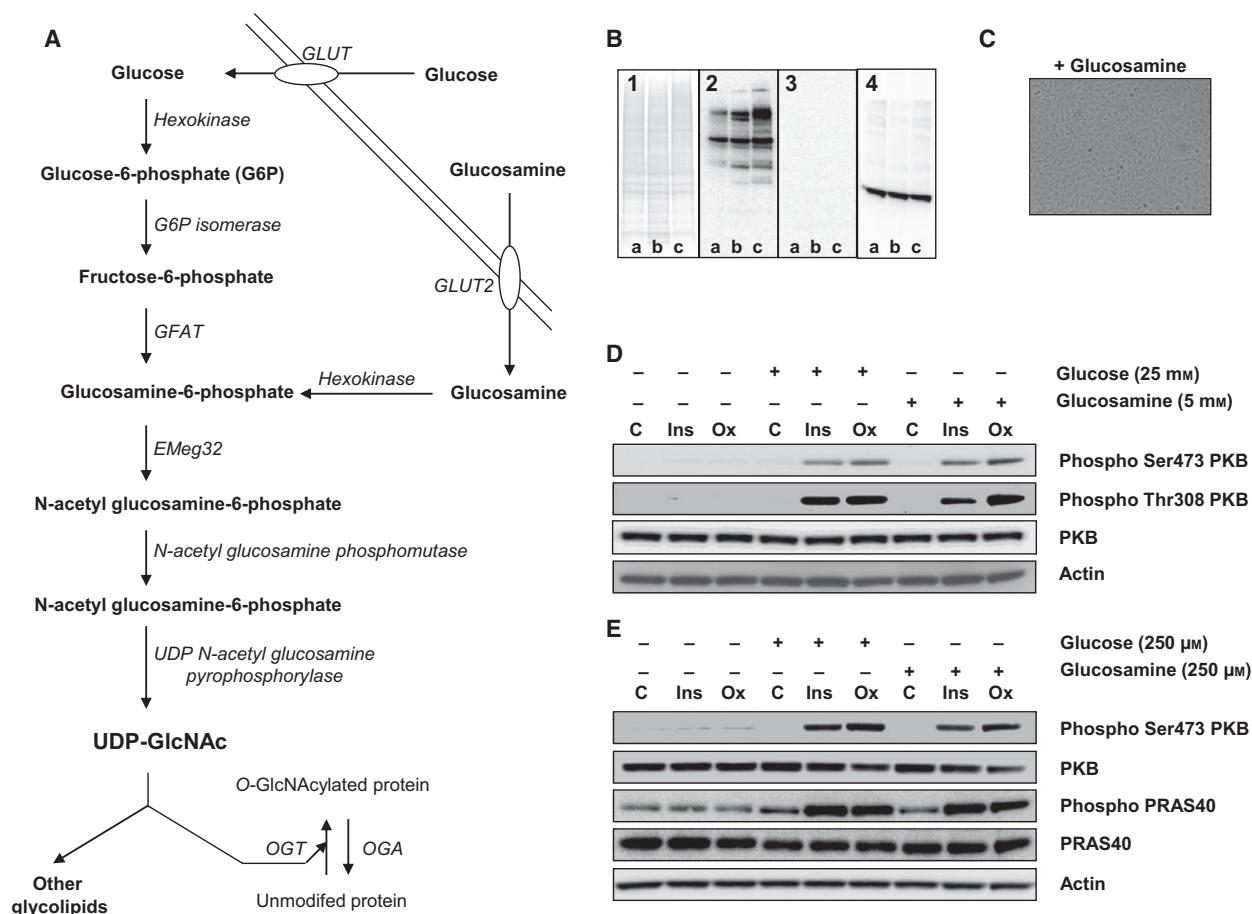


Fig. 2. (A) Schematic showing the HBP. Under normal conditions a small percentage of intracellular glucose enters the HBP to produce UDP-GlcNAc which is used by *O*-linked *N*-acetylglucosamine (*O*-GlcNAc) transferase (OGT) to modify serine and threonine residues on proteins. Removal of single *N*-acetylglucosamine from serine and threonine residues is accomplished by *O*-GlcNAcase (OGA). Glucosamine can enter into cells to feed the HBP below the level of the rate limiting step, that catalysed by glutamine fructose-6-phosphate amidotransferase (GFAT). (B) U2OS cells were plated in six-well plates using complete medium. The next day the cells were washed four times with NaCl/P_i before maintaining them for 6 h in serum- and glucose-free DMEM supplemented with nothing (lanes a), with 25 mM glucose (lanes b) or with 5 mM glucosamine (lanes c). Thereafter cell lysates were prepared. Panel 1: Coomassie Brilliant Blue stained gel. Panel 2: protein *O*-GlcNAc detection in cell lysates by western blotting. Panel 3: protein *O*-GlcNAc detection in cell lysates by western blotting (competition with 10 mM *N*-acetyl glucosamine). Panel 4: actin detection in cell lysates by western blotting. (C) U2OS cells were plated in six-well plates using complete medium. The next day the cells were washed four times with NaCl/P_i before maintaining them for 6 h in serum- and glucose-free DMEM supplemented with 5 mM glucosamine. A photograph was taken using a camera fitted to a microscope. (D) U2OS cells were plated in six-well plates using complete medium. The next day the cells were washed four times with NaCl/P_i before maintaining them for 6 h in serum- and glucose-free DMEM supplemented with nothing, with 25 mM glucose or with 5 mM glucosamine. The cells were control-treated, treated with 1 μg·mL⁻¹ insulin or treated with 1 mM H₂O₂ for 15 min. Thereafter cell lysates were prepared and western blotting was performed using the indicated antibodies. (E) U2OS cells were plated in six-well plates using complete medium. The next day the cells were washed four times with NaCl/P_i before maintaining them for 6 h in serum- and glucose-free DMEM supplemented with nothing, with 250 μM glucose or with 250 μM glucosamine. The cells were control-treated, treated with 1 μg·mL⁻¹ insulin or treated with 1 mM H₂O₂ for 15 min. Thereafter cell lysates were prepared and western blotting was performed using the indicated antibodies. Representative photographic images and western blots are shown. C, control; Ins, insulin; Ox, oxidative stress delivered in the form of H₂O₂.

incubation in the presence of 10 mM *N*-acetylglucosamine (Fig. 2B). As cells maintained in glucosamine appeared morphologically similar to cells maintained in glucose (Fig. 2C, compared with Fig. 1B) and have

comparable protein *O*-GlcNAc profiles (Fig. 2B), we next assessed PKB phosphorylation. Both insulin- and H₂O₂-mediated PKB phosphorylation, which was attenuated by glucose deprivation, was rescued by the

addition of exogenous glucosamine (Fig. 2D). A lower concentration (250 μM) of glucosamine also rescued PKB phosphorylation (Fig. 2E). Glucosamine's ability to rescue PKB phosphorylation was functional as it enabled both insulin- and H_2O_2 -induced PRAS40 phosphorylation (Fig. 2E), which is an established downstream target for activated PKB.

As deprivation of glucose leads to a loss of cellular ATP levels, we determined whether glucosamine might function to maintain ATP levels. The level of intracellular ATP decreased upon glucose deprivation but this was not rescued by extracellular glucosamine (Fig. 3A). In accordance the decrease in intracellular ATP correlated with an increase in AMPK activity,

and increased AMPK activity was not blocked by the addition of extracellular glucosamine (Fig. 3B). These data are consistent with the inability of glucosamine to act as a cellular energy source. Glucose deprivation also reduces the flux through the PPP measured as a decrease in intracellular glutathione (GSH); however, this was not rescued by glucosamine addition (Fig. 3C). In fact glucosamine decreased the ability of cells to reduce Alamar Blue (Fig. 3D) suggesting that it inhibits flux through the PPP. In summary, short-term glucose deprivation attenuates long-term cell growth and inhibits both insulin- and H_2O_2 -induced activation of PKB. Exogenously added glucosamine enables insulin- and H_2O_2 -mediated PKB activation

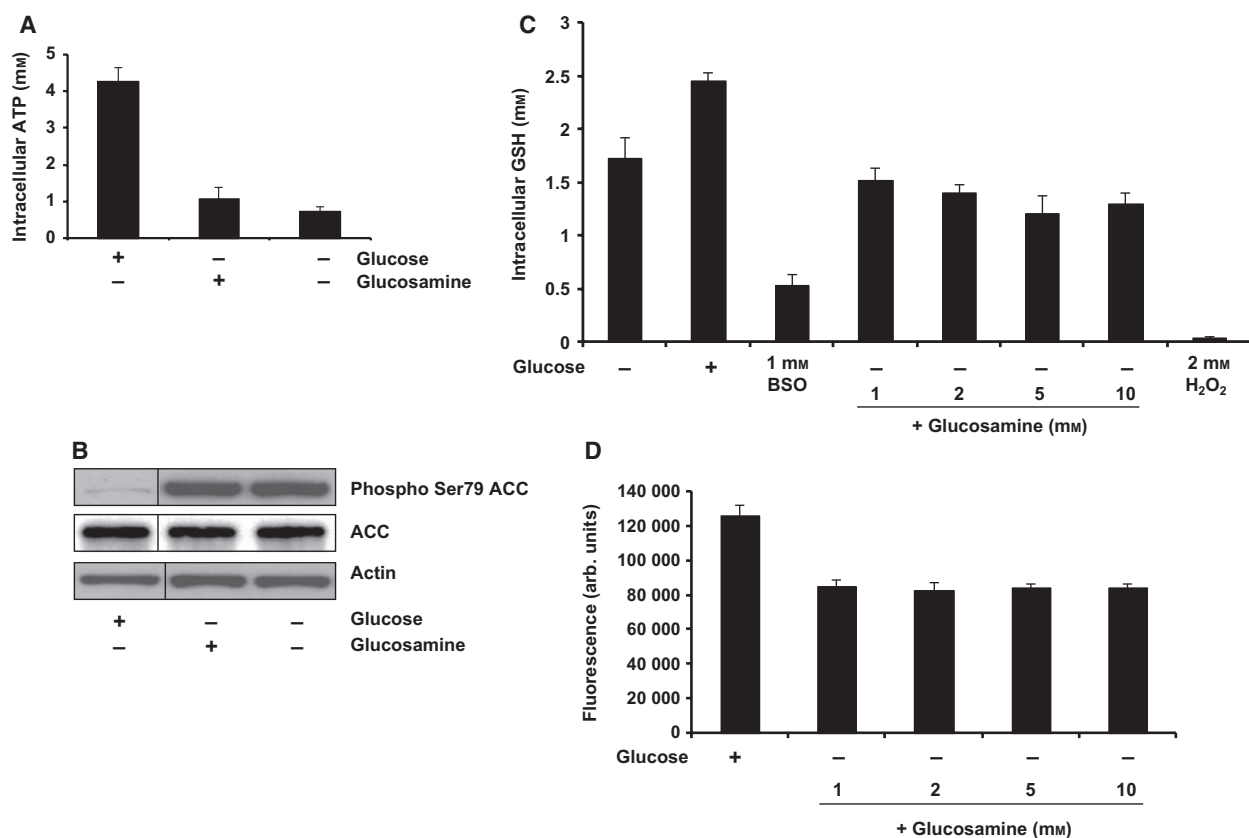


Fig. 3. (A) U2OS cells were plated in 96-well plates using complete medium. The next day the cells were washed four times with NaCl/P_i before maintaining them for 6 h in serum- and glucose-free DMEM supplemented as indicated. Intracellular ATP was measured using a kit. The graph shows the mean \pm SD ($n = 3$). (B) U2OS cells were plated in six-well plates using complete medium. The next day the cells were washed four times with NaCl/P_i before maintaining them for 6 h in serum- and glucose-free DMEM supplemented as indicated. Cell lysates were prepared and western blotting was performed using the indicated antibodies. Representative western blots are indicated. (C) U2OS cells were plated in 96-well plates using complete medium. The next day the cells were washed four times with NaCl/P_i before maintaining them for 6 h in serum- and glucose-free DMEM supplemented as indicated. Treatments with buthionine sulfoximine (BSO) and hydrogen peroxide (H_2O_2) were performed in glucose-containing DMEM. Intracellular GSH was measured using a kit. The graph shows the mean \pm SD ($n = 3$). (D) U2OS cells were plated in 96-well plates using complete medium. The next day the cells were washed four times with NaCl/P_i before maintaining them for 6 h in serum- and glucose-free DMEM supplemented as indicated. Alamar Blue reduction was monitored by measuring fluorescence. The graph shows the mean \pm SD ($n = 3$).

specific for phosphoinositide-dependent protein kinase 1 (PKB) (Fig. 4B). The ability of mTORC2 to phosphorylate PKB Ser473 in cells maintained in glucose-free medium supplemented with glucosamine was not affected by treatment of the cells with either rapamycin or metformin, two agents that impact on mTORC1 activity (Fig. 4C). Our results clearly indicate that mTORC2 and PDK1 are upstream kinases for PKB in U2OS cells stimulated in the presence of either glucose or glucosamine. The data suggest that glucosamine addition might bypass a nutrient sensor pathway that prevents PKB activation in the absence of glucose. We next assessed if bypass of nutrient sensors might be a universal feature of increased extracellular glucosamine. In the absence of amino acids, insulin no longer activates mTORC1 to induce phosphorylation and activation of S6K as assessed by Thr389 phosphorylation of p70S6K (Fig. 4D). However, extracellular glucosamine addition did not rescue p70S6K phosphorylation. We conclude that extracellular glucosamine bypasses a nutrient sensor pathway to enable activation of both PDK1 and mTORC2 to regulate PKB activity during glucose deprivation.

The HBP regulates PKB phosphorylation during glucose depletion and restriction

How might the addition of extracellular glucosamine regulate PKB activation? Extracellular glucosamine enters cells and increases the flux through the HBP (Fig. 2A). Flux through the HBP leads to an increase in UDP-GlcNAc, which can be used to synthesize glycoaminoglycans, glycolipids and complex glycosylated proteins. UDP-GlcNAc is also the substrate for OGT that transfers GlcNAc to protein serine residues. This step of the HBP provides a link between the biosynthesis of hexosamines and a signal transduction step. Glucosamine-mediated rescue of PKB phosphorylation was not inhibited by incubation with tunicamycin suggesting that *N*-glycosylation is not required (Fig. 5A). We therefore tested if protein *O*-GlcNAcylation might be required. Knockdown of OGT was carried out using lentiviral small hairpin RNA (shRNA) and was functionally assessed by monitoring protein *O*-GlcNAcylation. One cell line (shOGT¹) showed severely attenuated levels of *O*-GlcNAcylated proteins (20%–30%) compared with the control cell line (ShX) in the presence of high extracellular glucose. The other cell line (shOGT²) contained a higher level of *O*-GlcNAcylated proteins, with ~ 50% remaining, compared with ShX (Fig. 5B). In the absence of glucose but in the presence of extracellular glucosamine, both insulin- and H₂O₂-induced PKB phosphorylation was blunted (Ser473

PKB phosphorylation by ~ 70%, $P < 0.05$; Thr308 PKB phosphorylation by ~ 50%, $P < 0.05$) in shOGT¹ cells (Fig. 5B). This indicated that OGT-mediated *O*-GlcNAcylation is required for glucosamine to maintain PKB phosphorylation in response to insulin and H₂O₂. We next assessed if *O*-GlcNAcylation is required for insulin- and H₂O₂-induced PKB phosphorylation in the presence of high glucose levels. Although shOGT¹ and shOGT² cells exhibited reduced *O*-GlcNAcylation, PKB signalling was not attenuated in response to either insulin or H₂O₂ (Fig. 5C) in high glucose. We next reduced the levels of glucose and tested the role of the OGT in maintaining H₂O₂-induced PKB activation. As little as 15.6 μ M glucose permitted Ser473 PKB phosphorylation in response to H₂O₂; however, under these conditions OGT knockdown now attenuated PKB activation (Fig. 5D). At all three low concentrations of glucose (15.6 μ M, 31.25 μ M and 62.5 μ M) Ser473 PKB phosphorylation was significantly decreased when OGT was reduced (Fig. 5D).

We next assessed if extracellular glucosamine could enhance PKB activation in conditions of restricted flux through the HBP. Extracellular glucosamine addition to cells maintained in low glucose increased flux through the HBP as assessed by the amount of protein *O*-GlcNAcylation (Fig. 5E) and, more importantly, enhanced insulin-induced PKB phosphorylation at both Ser473 and Thr308. The effect on H₂O₂-induced PKB phosphorylation was less pronounced. No appreciable change in the phosphorylation of p38 in response to H₂O₂ stimulation was observed, illustrating the specificity of glucosamine in enhancing PKB phosphorylation (Fig. 5E). These data indicated that under conditions of restricted glucose protein *O*-GlcNAcylation becomes rate limiting for the activation of PKB by insulin and oxidative stress.

Rescue of insulin- and H₂O₂-mediated PKB phosphorylation during glucose deprivation by exogenously added glucosamine is dependent on the insulin receptor

How might enhanced OGT activity enable PKB signalling in restricted extracellular glucose? Enhanced OGT signalling might lead to post-translational modification of components of the insulin signalling pathway which would enable PKB signalling. OGT and *O*-GlcNAcylation also have a direct function in regulating gene transcription which might also impact on insulin signalling. We first deprived cells of glucose for 6 h in the absence of glucosamine and then switched the cells into medium containing extracellular glucosamine. At time points thereafter cells were stimulated with either

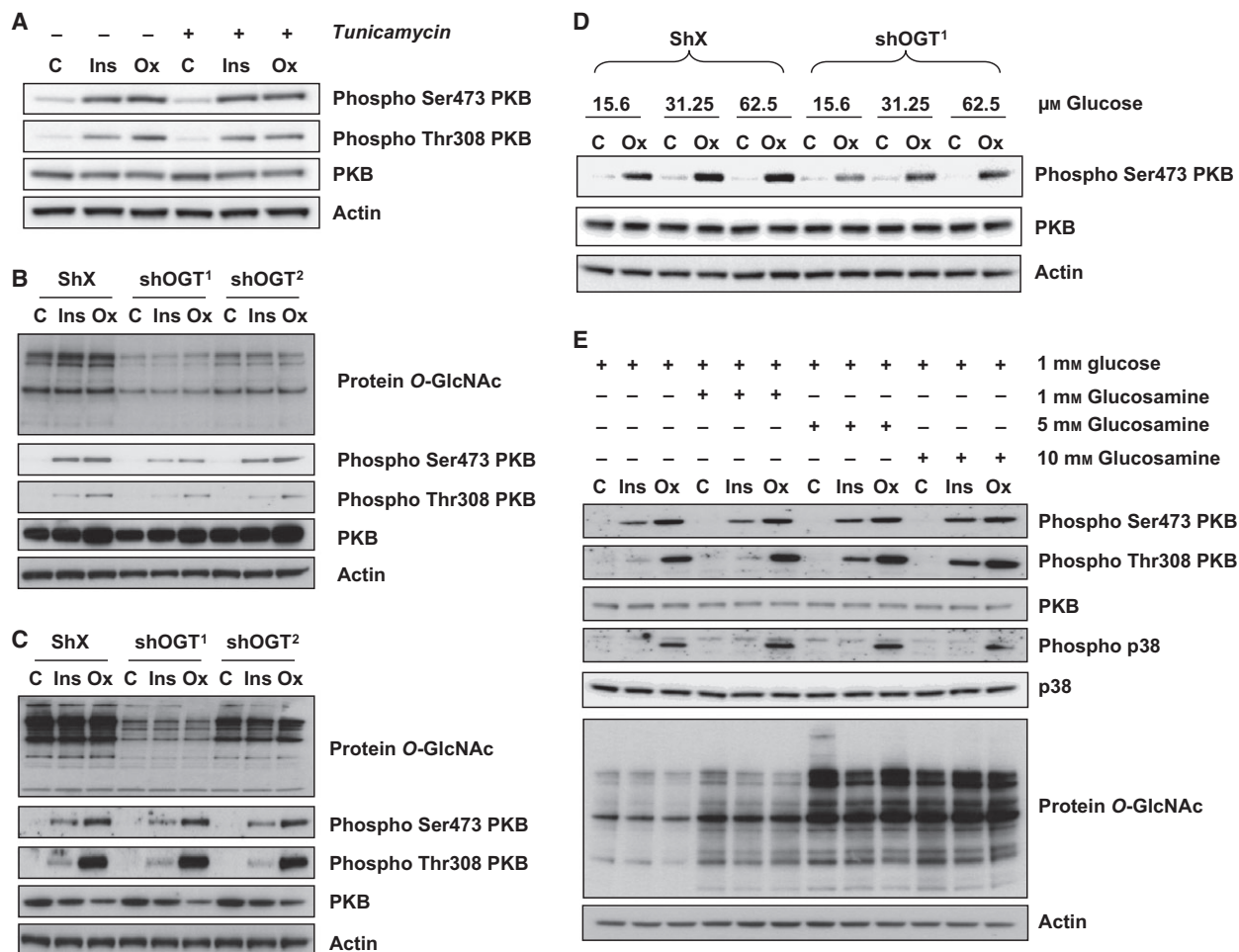


Fig. 5. (A) U2OS cells were plated in six-well plates using complete medium. The next day the cells were washed four times with NaCl/P_i before maintaining them for 6 h in serum- and glucose-free DMEM supplemented with 5 mM glucosamine in the absence or presence of tunicamycin (2 µM). Thereafter, the cells were control-treated, treated with 1 µg·mL⁻¹ insulin or treated with 1 mM H₂O₂ for 15 min. Cell lysates were prepared and western blotting was performed using the indicated antibodies. (B) ShX, shOGT¹ and shOGT² cells were plated in six-well plates using complete medium. The next day the cells were washed four times with NaCl/P_i before maintaining them for 6 h in serum- and glucose-free DMEM supplemented with 5 mM glucosamine. The cells were control-treated, treated with 1 µg·mL⁻¹ insulin or treated with 1 mM H₂O₂ for 15 min. Thereafter cell lysates were prepared and western blotting was performed using the indicated antibodies. (C) ShX, shOGT¹ and shOGT² cells were plated in six-well plates using complete medium. The next day the cells were washed four times with NaCl/P_i before maintaining them for 6 h in serum- and glucose-free DMEM supplemented with 25 mM glucose. The cells were control-treated, treated with 1 µg·mL⁻¹ insulin or treated with 1 mM H₂O₂ for 15 min. Thereafter cell lysates were prepared and western blotting was performed using the indicated antibodies. (D) ShX and shOGT¹ cells were plated in six-well plates using complete medium. The next day the cells were washed four times with NaCl/P_i before maintaining them for 6 h in serum- and glucose-free DMEM supplemented with very low concentrations of glucose as indicated. The cells were control-treated or treated with 1 mM H₂O₂ for 15 min. Thereafter cell lysates were prepared and western blotting was performed using the indicated antibodies. (E) U2OS cells were plated in six-well plates using complete medium. The next day the cells were washed four times with NaCl/P_i before maintaining them for 6 h in serum- and glucose-free DMEM supplemented with 1 mM glucose with increasing concentrations of glucosamine as indicated. The cells were control-treated, treated with 1 µg·mL⁻¹ insulin or treated with 1 mM H₂O₂ for 15 min. Thereafter cell lysates were prepared and western blotting was performed using the indicated antibodies. Representative western blots are indicated. C, control; Ins, insulin; Ox, oxidative stress delivered in the form of H₂O₂.

insulin or H₂O₂ and PKB phosphorylation was analysed. As expected, in the absence of both extracellular glucose and glucosamine PKB phosphorylation was modest (Fig. 6A); however, after as little as 30 min in

the presence of glucosamine, we observed increased PKB phosphorylation in response to both insulin and H₂O₂ suggesting that receptor proximal events rather than changes in gene transcription might underlie the

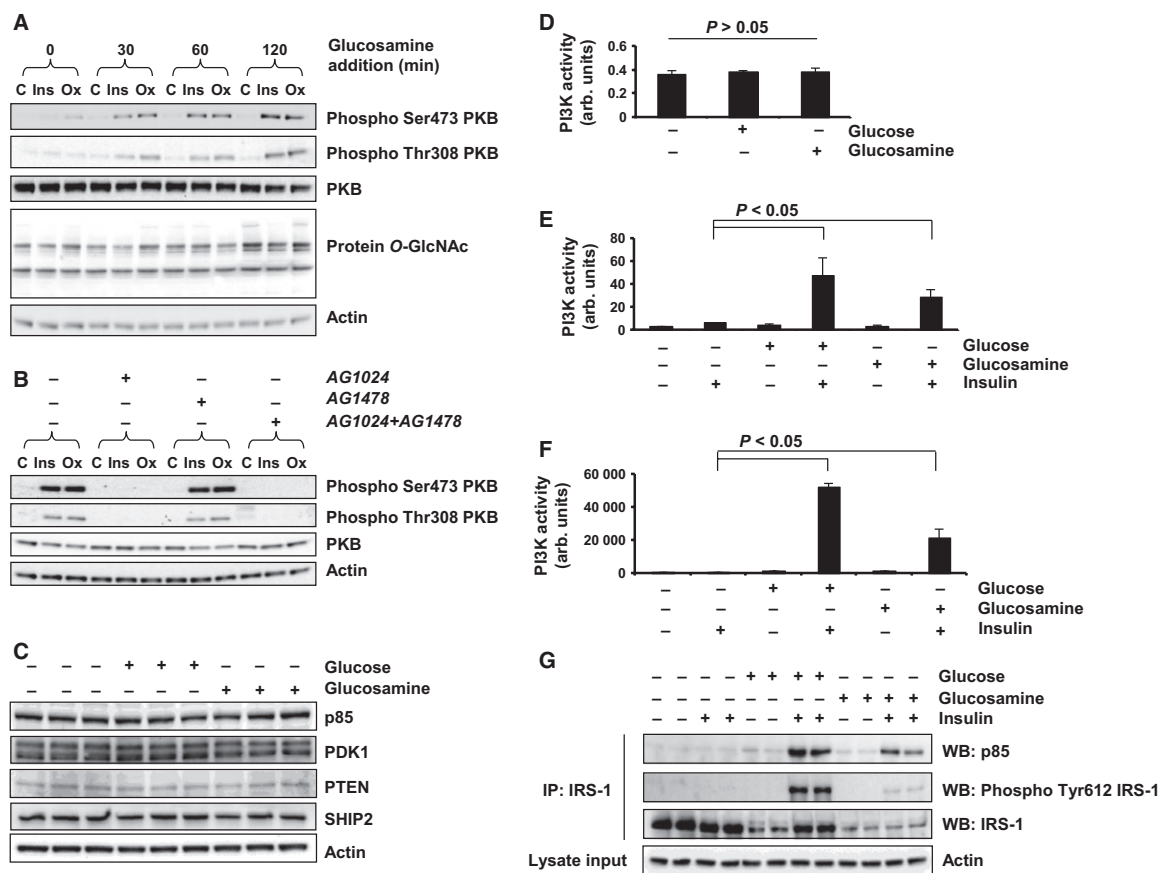


Fig. 6. (A) U2OS cells were plated in six-well plates using complete medium. The next day the cells were washed four times with NaCl/P_i before maintaining them for 6 h in serum- and glucose-free DMEM. Some cells were control-treated, treated with 1 $\mu\text{g}\cdot\text{mL}^{-1}$ insulin or treated with 1 mM H₂O₂ for 15 min. Other cells were treated with 5 mM glucosamine for the times indicated (after the initial 6 h incubation in serum- and glucose-free DMEM) prior to being control-treated, treated with 1 $\mu\text{g}\cdot\text{mL}^{-1}$ insulin or treated with 1 mM H₂O₂ for 15 min. Thereafter cell lysates were prepared and western blotting was performed using the indicated antibodies. (B) U2OS cells were plated in six-well plates using complete medium. The next day the cells were washed four times with NaCl/P_i before maintaining them for 6 h in serum- and glucose-free DMEM supplemented with 5 mM glucosamine containing dimethylsulfoxide (vehicle control for the tyrosinostats), 2 μM AG1024, 2 μM AG1478 or 2 μM AG1024 plus 2 μM AG1478. The cells were control-treated, treated with 1 $\mu\text{g}\cdot\text{mL}^{-1}$ insulin or treated with 1 mM H₂O₂ for 15 min. Thereafter cell lysates were prepared and western blotting was performed using the indicated antibodies. (C) U2OS cells were plated in six-well plates using complete medium. The next day the cells were washed four times with NaCl/P_i before maintaining them for 6 h in serum- and glucose-free DMEM supplemented as indicated. Thereafter cell lysates were prepared and western blotting was performed using the indicated antibodies. (D) U2OS cells were plated in six-well plates using complete medium. The next day the cells were washed four times with NaCl/P_i before maintaining them for 6 h in serum- and glucose-free DMEM supplemented as indicated. The cells were lysed and p85 was immunoprecipitated. Half of the immunoprecipitate was used to determine the level of p85 and the other half was used to measure PI3K activity using phosphatidylinositol as a substrate. The graph shows normalized PI3K activity (mean \pm SD, $n = 3$). (E) U2OS cells were plated in six-well plates using complete medium. The next day the cells were washed four times with NaCl/P_i before maintaining them for 6 h in serum- and glucose-free DMEM supplemented as indicated. The cells were control-treated or insulin-treated (1 $\mu\text{g}\cdot\text{mL}^{-1}$) in duplicate for 15 min. The cells were lysed and tyrosine phosphorylated proteins were immunoprecipitated. PI3K activity within the immunoprecipitates was determined. The graph shows PI3K activity (mean \pm SD, $n = 2$). (F) U2OS cells were plated in six-well plates using complete medium. The next day the cells were washed four times with NaCl/P_i before maintaining them for 6 h in serum- and glucose-free DMEM supplemented as indicated. The cells were control-treated or insulin-treated (1 $\mu\text{g}\cdot\text{mL}^{-1}$) in duplicate for 15 min. The cells were lysed and IRS-1 was immunoprecipitated. PI3K activity within the immunoprecipitates was determined. The graph shows PI3K activity (mean \pm SD, $n = 2$). (G) U2OS cells were plated in six-well plates using complete medium. The next day the cells were washed four times with NaCl/P_i before maintaining them for 6 h in serum- and glucose-free DMEM supplemented as indicated. The cells were control-treated or insulin-treated (1 $\mu\text{g}\cdot\text{mL}^{-1}$) in duplicate for 15 min. The cells were lysed and IRS1 was immunoprecipitated. Western blotting for p85, phospho-Tyr612 IRS-1 and IRS-1 was performed. Note that the total amount of IRS-1 immunoprecipitated was variable between the samples. Post-translational modification of IRS-1 is likely to affect the antibody's ability to recognize IRS-1. Acute changes (more than two-fold according to densitometry) in the level of IRS-1 between control and insulin-treated cells (lanes 5, 6, 7, 8) appear unlikely. Representative western blots are indicated. C, control; Ins, insulin; Ox, oxidative stress delivered in the form of H₂O₂.

glucosamine-mediated rescue of PKB activation (Fig. 6A). As glucosamine rescued both insulin- and H₂O₂-induced PKB activation we assessed whether H₂O₂ might function through activation of the insulin receptor using specific inhibitors directed against either the insulin/IGF1 receptor (AG1024) or the epidermal growth factor receptor (AG1478) as a control. AG1024 but not AG1478 attenuated both insulin's and H₂O₂'s ability to stimulate PKB phosphorylation (Fig. 6B), indicating the importance of insulin/IGF1 receptor tyrosine kinase activity in oxidative stress signalling.

The speed of recovery of PKB phosphorylation after the glucosamine switch and the fact that H₂O₂ functions through the insulin/IGF1 receptor led us to investigate early signalling events elicited by insulin. Furthermore as glucose deprivation attenuated both Ser473 and Thr308 phosphorylation, which are regulated by two different protein kinases, it was likely that an event upstream of both kinases was deregulated by glucose deprivation. Increased PtdIns(3,4,5)P₃ synthesis is essential for insulin-induced PKB activation and deregulated expression of components required for the generation/removal of 3-phosphoinositides might be responsible for attenuated PKB phosphorylation in the absence of glucose. Analysis of the expression of some insulin/PI3K components did not reveal any obvious changes that correlated with PKB activation: p85 (a PI3K signalling adaptor protein), PTEN [a PtdIns(3,4,5)P₃ 3-phosphatase], SHIP2 [a PtdIns(3,4,5)P₃ 5-phosphatase] and PDK1 (responsible for PKB Thr308 phosphorylation) (Fig. 6C). We also tested but did not find any changes in the total cellular levels of p85-associated PI3K (Fig. 6D). Insulin mediates PI3K activation through tyrosine phosphorylation which can be monitored as an increase in PI3K activity associated with protein phospho-tyrosine immunoprecipitates (Fig. 6E). Glucose restriction completely attenuated the association of PI3K activity with phospho-tyrosine immunoprecipitates, which was rescued by the addition of extracellular glucosamine (Fig. 6E). Next we measured PI3K activity associated with IRS-1 immunoprecipitates. Insulin strongly increased PI3K activity associated with IRS-1 immunoprecipitates, which was lost when cells were deprived of glucose (Fig. 6F) and was substantially rescued by the addition of extracellular glucosamine (Fig. 6F). We next assessed the level of IRS-1 phosphorylation at Tyr612 which is the docking site for p85 and the association of p85 with IRS-1. Insulin strongly stimulated both Tyr612 phosphorylation and the association of p85 with IRS1 but both were severely diminished in cells deprived of glucose (Fig. 6G). Both were substantially

rescued by the addition of extracellular glucosamine (Fig. 6G). These data are consistent with the loss of proximal insulin receptor tyrosine kinase signalling in cells by glucose deprivation which can be rescued by the addition of glucosamine. This suggests that under conditions of low extracellular glucose *O*-GlcNAcylation can maintain insulin-driven tyrosine kinase signalling to activate PI3K.

Insulin- and H₂O₂-stimulated 3-phosphoinositide production requires extracellular glucose or glucosamine

The previous data suggest that deprivation of glucose attenuates insulin-driven PI3K activation. We therefore examined 3-phosphorylated phosphoinositide production in response to both insulin and H₂O₂ stimulation. U2OS cells were maintained in the presence and absence of glucose or in the absence of glucose with the addition of extracellular glucosamine for 6 h after which they were stimulated with insulin. Both basal and insulin-stimulated PtdIns(3,4,5)P₃ molecular species were quantitated by LC-MS/MS. Insulin increased the level of 38:4, 38:3, 36:2, 36:1 PtdIns(3,4,5)P₃ species but this increase was severely reduced in the absence of glucose (Fig. 7A). The loss of insulin-induced PtdIns(3,4,5)P₃ was rescued by the addition of extracellular glucosamine. Merged data from Fig. 7A are shown in Fig. 7B. H₂O₂ can activate PKB through the generation of phosphatidylinositol(3,4)-bisphosphate [PtdIns(3,4)P₂], and as LC-MS/MS is unable to accurately quantitate PtdIns(3,4)P₂ we monitored its production *in vivo* using metabolic radiolabelling with [³²P]-orthophosphate. Treatment of the cells with H₂O₂ caused the production of PtdIns(3,4)P₂ in cells maintained in either glucose or glucosamine (Fig. 7C). These data demonstrate that glucose deprivation attenuates insulin- and H₂O₂-induced synthesis of 3-phosphorylated lipids and that this can be rescued by the addition of extracellular glucosamine.

Inhibition of long-term cell growth by a brief period of glucose deprivation is overcome by inclusion of exogenous glucosamine

Previous work from our laboratory demonstrated that the growth of U2OS cells was highly dependent on the PI3K/mTOR/PKB pathway [34]. Glucose-deprived U2OS cells have attenuated insulin-stimulated PI3K/PKB signalling, which can be rescued by increasing the flux through the HBP. We therefore assessed whether glucosamine could rescue the observed inhibition of

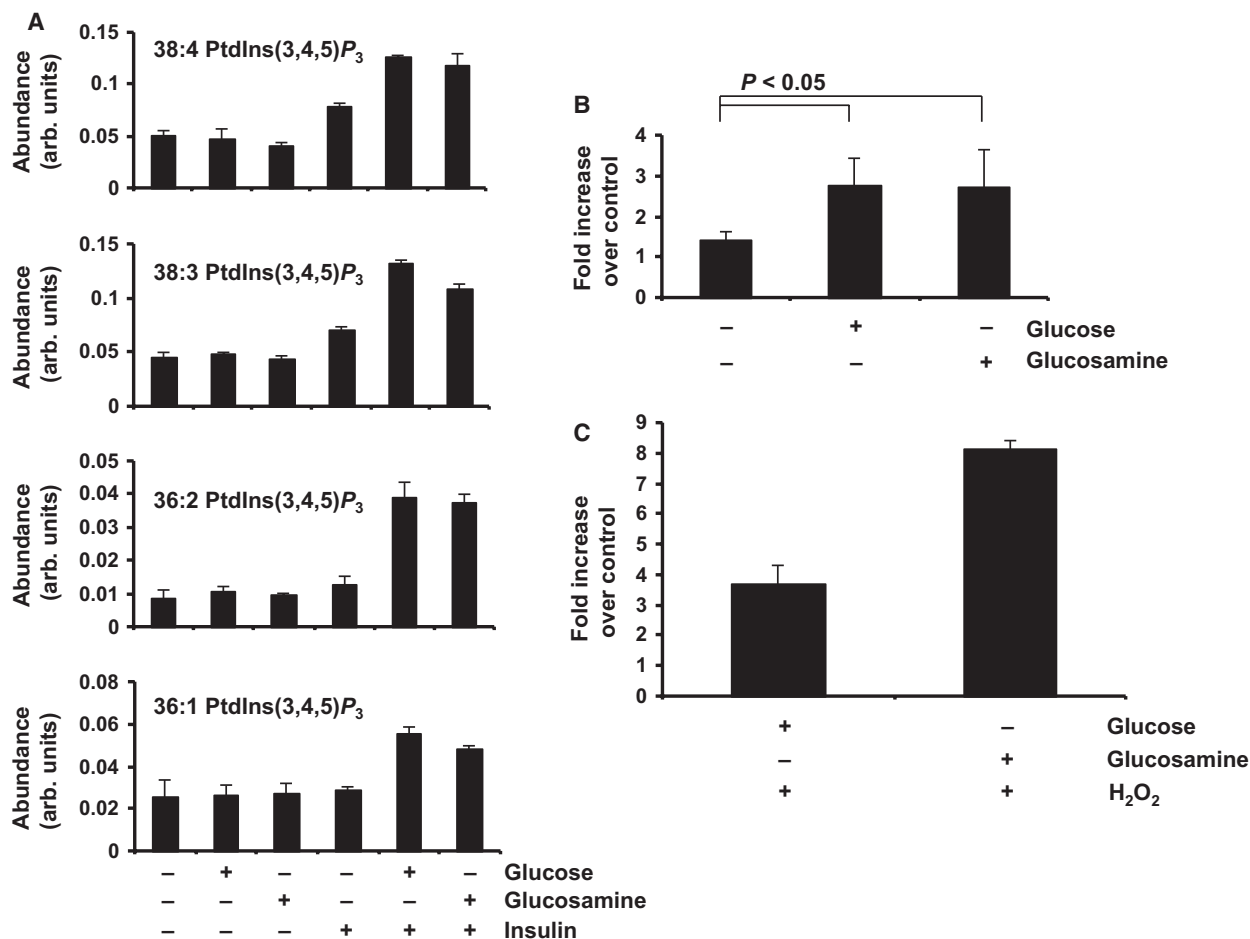


Fig. 7. (A) U2OS cells were plated in six-well plates using complete medium. The next day the cells were washed four times with NaCl/P_i before maintaining them for 6 h in serum- and glucose-free DMEM supplemented with nothing, with 25 mM glucose or with 5 mM glucosamine. The cells were control-treated or treated with 1 $\mu\text{g}\cdot\text{mL}^{-1}$ insulin for 15 min. The medium overlying the cells was rapidly removed, the monolayer was quickly washed once with NaCl/P_i and the incubations were quenched by the addition of 1 mL of ice-cold 1 M HCl. Cellular material was used for PtdIns(3,4,5)P₃ analysis. Graphs for individual PtdIns(3,4,5)P₃ isomers are illustrated. (B) Summary graph combining data from the individual PtdIns(3,4,5)P₃ isomers (from A). (C) U2OS cells were plated in six-well plates using complete medium. The next day the cells were washed four times with NaCl/P_i before maintaining them for 6 h in serum- and glucose-free DMEM supplemented with either 25 mM glucose or 5 mM glucosamine. Thereafter the cells were washed with HEPES-buffered saline supplemented with either 25 mM glucose or 5 mM glucosamine prior to incubation in metabolic radiolabelling medium. The cells were control-treated or treated with 1 mM H₂O₂ for the times indicated. Total lipid extracts were deacylated and the glycerophospho headgroups were separated by SAX-HPLC. The radioactivity in PtdIns(3,4)P₂ was normalized to that found in phosphatidylinositol 3-phosphate (PtdIns3P). The radioactivity incorporated into the latter was found not to change in response to any treatments or cell culture conditions. The graph represents mean \pm SD ($n = 3$).

cell growth induced by short-term glucose deprivation (Fig. 1A). Cells were plated at low density and were maintained in the presence or absence of glucose or in the absence of glucose supplemented with glucosamine for 6 h before being returned to normal culture conditions (containing serum and glucose). As observed previously (Fig. 1A) short-term glucose deprivation completely attenuated long-term cell growth (Fig. 8A). In accordance with increased flux through the HBP

maintaining PKB activation, short-term glucosamine incubation almost completely rescued cell growth inhibition by glucose deprivation (Fig. 8A). We next assessed whether protein *O*-GlcNAcylation was required for glucose-mediated cell growth. At quite low concentrations of extracellular glucose (125 μM), OGT knockdown did not affect long-term cell growth (Fig. 8B). However, at very low concentrations of glucose inhibition of *O*-GlcNAcylation by OGT

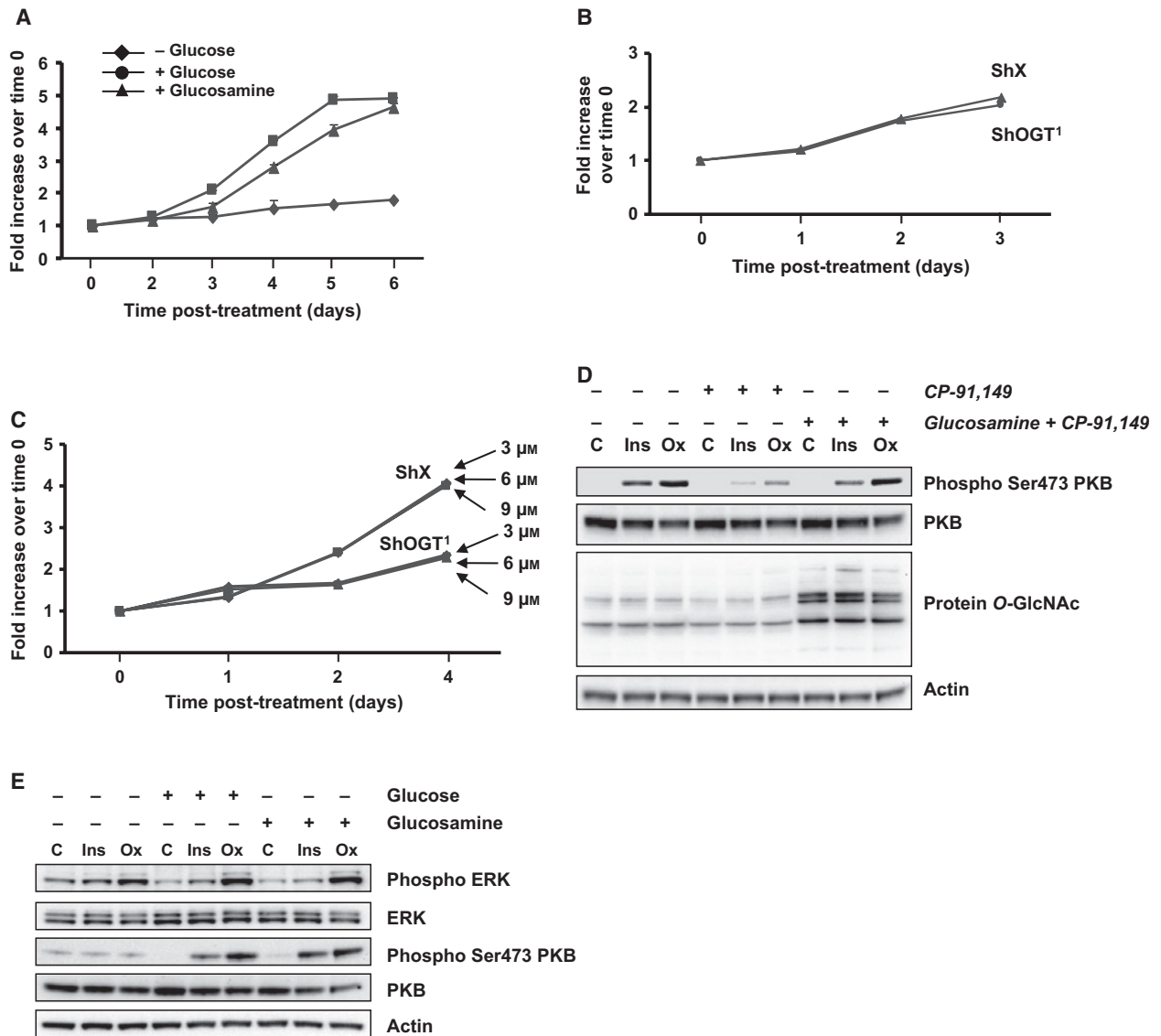


Fig. 8. (A) U2OS cells were plated at low density (30 000 per well) in six-well plates using complete medium. The next day the cells were washed four times with NaCl/P_i before maintaining them for 6 h in serum- and glucose-free DMEM supplemented with nothing, with 25 mM glucose or with 5 mM glucosamine followed by media removal and replacement with serum- and glucose-containing DMEM. At intervals thereafter, cell monolayers were washed twice with NaCl/P_i before staining with crystal violet. Crystal violet stain was solubilized and quantitated by spectrophotometry. The graph represents mean \pm SD ($n = 3$). Error bars are within the size of the line symbols. (B) ShX and ShOGT¹ were plated at low density (30 000 per well) in six-well plates using complete medium. The next day the cells were washed four times with NaCl/P_i before maintaining them for 6 h in serum- and glucose-free DMEM supplemented with low glucose (125 μ M) followed by media removal and replacement with serum- and glucose-containing DMEM. At intervals thereafter, cell monolayers were washed twice with NaCl/P_i before staining with crystal violet. Crystal violet stain was solubilized and quantitated by spectrophotometry. The graph represents mean \pm SD ($n = 3$). Error bars are within the size of the line symbols. (C) As (B) except that very low glucose concentrations (3 μ M, 6 μ M and 9 μ M) were used. (D) A549 cells were plated in six-well plates using complete medium. The next day the cells were washed four times with NaCl/P_i before maintaining them for 6 h in serum- and glucose-free DMEM supplemented with 30 μ M glucose in the presence or absence of 20 μ M CP-91,149 and 5 mM glucosamine as indicated. The cells were control-treated, treated with 1 μ g·mL⁻¹ insulin or treated with 1 mM H₂O₂ for 15 min. Thereafter cell lysates were prepared and western blotting was performed using the indicated antibodies. (E) U2OS cells were plated in six-well plates using complete medium. The next day the cells were washed four times with NaCl/P_i before maintaining them for 6 h in serum- and glucose-free DMEM supplemented as indicated. The cells were control-treated, treated with 1 μ g·mL⁻¹ insulin or treated with 1 mM H₂O₂ for 15 min. Thereafter cell lysates were prepared and western blotting was performed using the indicated antibodies. Representative western blots are indicated. C, control; Ins, insulin; Ox, oxidative stress delivered in the form of H₂O₂.

knockdown strongly reduced cell growth (Fig. 8C). These data are consistent with the requirement of the HBP and OGT pathway for long-term cell growth when cells experience limiting glucose conditions for short periods.

In many types of tumour cells inhibition of cell proliferation and survival induced by glucose deprivation is overcome in the short term by an increase in glycogenolysis. In fact the growth of many tumour cells is sensitive to inhibition of glycogen breakdown [39,40]. In A549 cells glycogen-derived glucose released under conditions of glucose deprivation is fed directly into the HBP in order to maintain protein *O*-GlcNAcylation and cell growth and inhibition of glycogen phosphorylase by CP91-149 strongly inhibits A549 cell growth [39,40]. Drawing on these observations and the data from this study, we investigated PKB activation in A549 cells under limiting glucose availability. Under glucose-restrictive conditions (0.03 mM glucose) the ability of both insulin and H₂O₂ to stimulate PKB phosphorylation in A549 cells was severely impaired when cells were treated with CP91-149 (Fig. 8D). To implicate the requirement for the HBP, we added glucosamine to CP91-149-treated A549 cells. Under these conditions glucosamine bypassed the requirement for glycogen breakdown for both insulin- and H₂O₂-induced PKB phosphorylation (Fig. 8D). This suggests that increased glycogenolysis can be used to fuel the HBP under restrictive glucose conditions to maintain receptor-induced PKB signalling.

Discussion

While the mTORC1 pathway is known to respond to changes in extracellular nutrients, much less is known about how nutrients might regulate the PI3K/PKB pathway. We show that short-term glucose deprivation uncouples insulin/IGF1 receptor stimulation from the activation of the PI3K/PKB pathway. The uncoupling occurs proximal to the receptor and leads to the inhibition of tyrosine phosphorylation of IRS-1, IRS-1-mediated recruitment of the PI3K complex and PtdIns(3,4,5)P₃ synthesis. Surprisingly, addition of extracellular glucosamine almost completely restores IRS-1 phosphorylation leading to increased PtdIns(3,4,5)P₃ generation and the activation of PKB in response to both insulin and oxidative stress in the absence of extracellular glucose. Uncoupling of the activation of the PI3K/PKB pathway correlated with a reduction in long-term cell proliferation after glucose deprivation which was restored by extracellular glucosamine. Finally our studies suggest that enhanced glycogenolysis maintains insulin-receptor-mediated activation of

PKB through the maintenance of flux through the HBP.

Counterintuitively, a number of studies have demonstrated an increase in *O*-GlcNAcylation in response to glucose deprivation probably as a consequence of the activation of OGT, inhibition of OGA or through increased glycogenolysis to fuel the HBP [39,41,42]. These data suggest a functional requirement for increased *O*-GlcNAcylation during glucose restriction/deprivation. In U2OS cells glucose deprivation did not lead to an increase in *O*-GlcNAcylation but instead led to the attenuation of PKB activation in response to insulin/H₂O₂ and a loss of long-term proliferation, which could be rescued by extracellular glucosamine. Glucosamine was shown to anapleurally drive HBP flux without restoring cellular ATP levels. Glucosamine might drive an increase in both *N*- and *O*-glycosylation of proteins to maintain insulin receptor function. Both insulin and IGF1 receptors are heavily *N*-glycosylated and loss of specific sites of *N*-glycosylation attenuates receptor trafficking to the plasma membrane [28,29]. Although it is likely that glucose deprivation in U2OS cells attenuates *N*-glycosylation, tunicamycin treatment did not attenuate glucosamine-mediated rescue of insulin- and H₂O₂-mediated PKB phosphorylation. In addition, OGT knockdown implicated reduced *O*-GlcNAcylation in uncoupling receptor stimulation to activation of PI3K/PKB. Furthermore, short-term glucose starvation did not block insulin- and H₂O₂-mediated extracellular signal-regulated kinase phosphorylation, suggesting that some aspects of receptor signalling are still intact (Fig. 8E). These data support a role for *O*-GlcNAcylation in regulating early signalling events between receptor activation, IRS-1 phosphorylation, PI3K activation and PKB phosphorylation.

Many components of the insulin signalling pathway have been shown to be *O*-GlcNAcyated including the IR, IRS-1, PDK1 and PKB [43] and further studies will be required to understand exactly which components enable glucosamine-mediated PKB activation in the absence of glucose. How *O*-GlcNAcylation regulates insulin signalling and PKB activation is complex as flux through the HBP and protein *O*-GlcNAcylation pathway have been implicated in both the activation and inhibition of insulin-induced PKB activity. In adipocytes treatment with the OGA inhibitor PUGNAc, which increases *O*-GlcNAcylation, was shown to induce insulin resistance and decrease PKB activity [43–45], while in muscle PUGNAc induces insulin resistance but does not affect PKB activation [46]. However, other studies have shown that structurally unrelated but better inhibitors of OGA do not show a similar

phenotype to PUGNAc in adipocytes [47–49] suggesting that the effect of PUGNAc may be off-target. In *Caenorhabditis elegans* upregulation of the OGT pathway appears to inhibit insulin signalling [50,51], whilst in *Drosophila melanogaster* upregulation of *O*-GlcNAcylation stimulates insulin signalling [52]. These data suggest that *O*-GlcNAcylation affects insulin signalling in a cell-type-dependent manner. Interestingly in *C. elegans* knockdown of OGA induces hyper *O*-GlcNAcylation of histone tails associated with promoters and changes the expression of many genes involved in insulin signalling [51]. Therefore, the differences observed in various cell types might reflect a balance between how *O*-GlcNAcylation modifies long-term gene expression and short-term signalling outputs.

A strong candidate for transducing an *O*-GlcNAcylation signal to insulin signalling under glucose restrictive conditions is the IRS-1 protein. In response to insulin/IGF1, IRS-1 is tyrosine phosphorylated which recruits the PI3K complex and stimulates PtdIns(3,4,5) P_3 synthesis. IRS-1 is also phosphorylated and *O*-GlcNAcylated at several serine and threonine residues which contributes to the regulation of downstream targets [43,45,53,54]. For example IRS-1 serine/threonine phosphorylation induced by p38, AMPK or by hyperactivation of S6K inhibits insulin-mediated IRS-1 tyrosine phosphorylation and PtdIns(3,4,5) P_3 synthesis. How *O*-GlcNAcylation of IRS-1 might regulate combinatorial phosphorylation and IRS-1 signalling output is not clear, although as the sites of *O*-GlcNAcylation do not overlap with the sites of serine/threonine phosphorylation straightforward competition is unlikely to be relevant.

Evidence from this study supports a role for flux through the HBP in permitting insulin/IGF1 signalling to maintain PKB activation under conditions of glucose restriction and might reflect a requirement in cancer cells rather than in non-transformed differentiated adipocytes. Cancer cells rewire their metabolic programme to increase both glucose and glutamine utilization to sustain rapid proliferation rates [16] and to respond to changes in nutritional status. As the HBP pathway is driven by both these components it is plausible that increased *O*-GlcNAcylation might be critical for tumour cell proliferation. The growth of tumour cell lines *in vitro* and *in vivo* has been shown to be reduced in cells with reduced *O*-GlcNAcylation. For example in 8305C thyroid anaplastic cancer cells both basal and IGF1-stimulated PKB activation and cell proliferation are increased when *O*-GlcNAcylation is increased either pharmacologically or genetically [55]. Protein *O*-GlcNAcylation is also required for breast and pancreatic tumour cell growth [26,27]. Further-

more oncogenes such as Ras [25] or Myc [56] induce global increases in *O*-GlcNAcylation. These data together with the data in this study reinforce the concept that in cancer cells metabolic rewiring leads to increased HBP flux which participates in tumour cell growth under certain restrictive conditions.

Decreases in intracellular glucose in tumour cells can occur as a consequence of poor tumour vasculature [9] or by decreased glucose uptake as observed in tumour cells that lose matrix contact [57]. Under these conditions of glucose restriction, redirecting glycolytic intermediates to the HBP to increase *O*-GlcNAcylation might confer a temporary measure to maintain insulin/IGF1-mediated PKB activation and inhibit the induction of apoptosis. A likely source for increasing flux through the HBP is from cell glycogen and indeed glycogenolysis has been shown to be important for tumour cell growth under conditions of nutrient deprivation during hypoxia [10,40,58,59]. Furthermore, mild hypoxia increases glycogen synthesis which is essential for pre-conditioning tumour cells to withstand stronger hypoxic conditions [58,60]. Interestingly we show that under restricted glucose conditions glycogenolysis maintains insulin stimulation of the PKB pathway in A549 lung cancer cells and that it probably does so by providing fuel for the HBP pathway. Our studies suggest that specific inhibition of OGT might enhance tumour killing in combination with therapeutics that inhibit glucose uptake and utilization.

Materials and methods

Cell culture, treatments and western blotting

U2OS and A549 cells were maintained in culture using DMEM (Sigma, Dorset, UK) containing 25 mM glucose supplemented with 4 mM glutamine (Invitrogen, Paisley, UK) and 10% heat-inactivated fetal bovine serum (Sigma). For most experiments the cells were seeded in six-well plates. The next day the cells were washed four times with phosphate buffered saline (NaCl/P_i) before re-incubation in serum-free DMEM lacking glucose (Invitrogen). This minimal medium was supplemented with 25 mM glucose (Sigma) or with 5 mM glucosamine hydrochloride (Sigma) where indicated for 6 h. A stock solution of glucosamine was always prepared fresh on the day of experiments (100 mM glucosamine in glucose-free DMEM) and diluted as necessary. Glucose was undetectable in the 100 mM glucosamine stock solution. Photographs of the cells were taken using a Zeiss Axiovert 40CFL camera controlled by AXIOVISION software. In some experiments during the 6 h period of nutrient withdrawal the cells were incubated with inhibitors of specific pathways. Dimethylsulfoxide (or the appropriate vehicle) was always used as a control.

The inclusion of inhibitors is detailed in the relevant figure legends.

At the end of the 6 h the cells were challenged with insulin ($1 \mu\text{g}\cdot\text{mL}^{-1}$) or hydrogen peroxide (H_2O_2) (1 mM) for the times indicated in the figure legends. The incubations were quenched by the removal of medium from the well followed by rapid addition of $1 \times$ LDS/PAGE sample buffer (Invitrogen), 100 mM dithiothreitol (Sigma), lysis buffer (1% v/v NP-40, 50 mM Tris/HCl pH 8, 50 mM potassium chloride, 10 mM EDTA), protease inhibitor/protein phosphatase inhibitor cocktails (Roche, West Sussex, UK) and $100 \text{ U}\cdot\text{mL}^{-1}$ benzoylase nuclease (Sigma). After leaving on ice for 15 min the samples were collected and heated for 10 min at 70°C . Proteins in cell lysates were resolved by electrophoresis using 1 mm thickness 4–12% acrylamide Bis-Tris pre-cast gels (Invitrogen) and wet protein transfer to nitrocellulose membranes. All primary antibodies were purchased from Cell Signalling Technology (Hertfordshire, UK), Millipore (Hertfordshire, UK), Sigma and Santa Cruz and horseradish-peroxidase-coupled secondary antibodies were from GE Healthcare (Amersham, UK) and Santa Cruz. CP-91,149, tunicamycin, metformin and rapamycin were purchased from Sigma. Torin 2, AG1024 and AG1478 were purchased from SelleckChem.

Immunoprecipitations and PI3K assays

After 6-h incubations in different energy-providing media control and acutely stimulated cells were lysed in ice-cold 1% (v/v) NP-40 lysis buffer (for details see above) supplemented with protease inhibitor/protein phosphatase inhibitor cocktails, 1 mM sodium orthovanadate (Sigma), 1 mM beta-glycerophosphate (Sigma), 5 mM sodium fluoride (Sigma), $1 \mu\text{M}$ okadaic acid (Sigma) and $100 \text{ U}\cdot\text{mL}^{-1}$ benzoylase nuclease. After standing on ice for 15 min the lysates were cleared by centrifugation ($20\,000 g$ for 15 min at 4°C). Immunocomplexes were allowed to form overnight at 4°C . Protein G sepharose (Sigma) was used to precipitate complexes. After washing the immunoprecipitates four times with 50 mM Tris/HCl pH 7.5 containing 5 mM EDTA, 150 mM sodium chloride and 0.1% (v/v) Tween-20 the proteins were resolved by electrophoresis and detected by western blotting as detailed above. PI3K assays were performed using washed immunoprecipitates further washed with 50 mM Tris/HCl pH 7.4 containing 10 mM magnesium chloride, 1 mM EGTA and 70 mM potassium chloride. Kinase activity towards 1 nmol substrate diC_{16} -phosphatidylinositol (Cell Signalling) mixed with 10 nmol of phosphatidylserine (Sigma) in the presence of $20 \mu\text{M}$ ATP and $10 \mu\text{Ci}$ [^{32}P] γ -ATP (Perkin Elmer, Cambridgeshire, UK) was determined by the generation of radiolabelled phosphatidylinositol 3-phosphate (PtdIns3P) for 10 min at 30°C . Radiolabelled PtdIns3P was extracted and separated by TLC using silica gel 60 \AA $20 \times 20 \text{ cm}$ plates (Merck-Millipore). The TLC plates were run once

in chloroform/methanol/water/25% ammonia solution (45/35/8/2, v/v/v/v), air dried for 1 h and radioactivity in separated lipid spots was quantitated by phosphorimaging analysis (BioRad).

Metabolic labelling and phosphoinositide analysis

Following 5 h of incubation in differently supplemented DMEM U2OS cells were washed four times with phosphate-free HEPES-buffered saline containing amino acids (mixture of essential and non-essential amino acids) (Invitrogen). Metabolic radiolabelling was performed using phosphate-free HEPES-buffered saline containing amino acids supplemented with glucose or with glucosamine and $300 \mu\text{Ci}\cdot\text{mL}^{-1}$ [^{32}P]-labelled phosphate (Perkin Elmer) for the last 1 h. Metabolic radiolabelling was terminated by quenching cell monolayers with 1.2 M HCl followed by total lipid extraction (Bligh–Dyer method). Radiolabelled phosphoinositides were separated by TLC (as indicated above) or directly deacylated for HPLC analysis of the phosphoinositide headgroups. Non-radiolabelled PtdIns (3,4,5) P_3 measurements were performed as described previously [61].

ATP, GSH measurements and Alamar Blue reduction assay

U2OS cells were seeded in 96-well plates. The next day the cells were washed four times with NaCl/ P_i before incubation in differently supplemented DMEM for 6 h. Following the incubations intracellular ATP and GSH was measured using kits from Perkin Elmer and Promega (Southampton, UK), respectively. The cells' ability to reduce Alamar Blue (Invitrogen) was assessed by its direct addition to the wells for the last 3 h of incubation in the above-mentioned media. Fluorescence measurements were performed according to the manufacturer's instructions.

shRNA-mediated knockdown of OGT

Two OGT short hairpin (sh) targeting constructs GCTGAGCAGTATTCCGAGAAA and GCCCTAA GTTTGAGTCCAAAT (MISSION pLKO.1 shRNA clones TRCN0000035067 and TRCN0000035064, Sigma) were used to make two separate stable lentivirus-transduced OGT knockdown U2OS cell lines shOGT¹ and shOGT². A U2OS cell line made with the control-targeting construct CAACAAGATGAAGAGACCAA (MISSION[®] pLKO.1-puro Non-Mammalian shRNA Control Plasmid DNA targeting no known mammalian genes) was made in parallel. All three cell types were used simultaneously for experiments and were maintained in culture medium containing $2 \mu\text{g}\cdot\text{mL}^{-1}$ puromycin (Sigma).

Growth assays

U2OS cells were plated in six-well plates (30 000 per well) and left in complete medium for 24 h. The cells were then washed four times with NaCl/P_i prior to incubation in differently supplemented DMEM for 6 h. Thereafter, the media were removed and replaced with normal complete medium. At intervals thereafter, cell monolayers were washed twice with NaCl/P_i before staining with crystal violet solution (crystal violet 0.1% w/v; formaldehyde 4% v/v; methanol 50% v/v). The stained monolayers were washed and dried and the plates scanned. The crystal violet stain was removed from the wells using water/methanol/concentrated acetic acid (7:2:1, v/v/v) and the absorbance of the coloured solution was monitored at 618 nm.

Acknowledgements

We wish to thank all past and present members of the Inositide Laboratory for technical help and discussions during the course of the work. Financial support was entirely from Cancer Research UK. The authors disclose no potential conflicts of interest.

Author contributions

DRJ and WJK carried out the majority of experiments. LRS, KEA and PTH carried out the PIP3 measurements. Experiments were designed by DRJ and ND. The manuscript was written by DRJ and ND and all authors contributed to the final manuscript.

References

- Buchakjian M & Kornbluth S (2010) The engine driving the ship: metabolic steering of cell proliferation and death. *Nat Rev Mol Cell Biol* **11**, 715–727.
- Carling D, Thornton C, Woods A & Sanders MJ (2012) AMP-activated protein kinase: new regulation, new roles? *Biochem J* **445**, 11–27.
- Woods A, Johnstone SR, Dickerson K, Leiper FC, Fryer LG, Neumann D, Schlattner U, Wallimann T, Carlson M & Carling D (2003) LKB1 is the upstream kinase in the AMP-activated protein kinase cascade. *Curr Biol* **13**, 2004–2008.
- Shaw RJ & Cantley LC (2006) Ras, PI(3)K and mTOR signalling controls tumour cell growth. *Nature* **441**, 424–430.
- Shaw RJ, Bardeesy N, Manning BD, Lopez L, Kosmatka M, DePinho RA & Cantley LC (2004) The LKB1 tumor suppressor negatively regulates mTOR signaling. *Cancer Cell* **6**, 91–99.
- Shaw RJ, Kosmatka M, Bardeesy N, Hurley RL, Witters LA, DePinho RA & Cantley LC (2004) The tumor suppressor LKB1 kinase directly activates AMP-activated kinase and regulates apoptosis in response to energy stress. *Proc Natl Acad Sci U S A* **101**, 3329–3335.
- Wellen K & Thompson C (2010) Cellular metabolic stress: considering how cells respond to nutrient excess. *Mol Cell* **40**, 323–332.
- Guarente L (2011) The logic linking protein acetylation and metabolism. *Cell Metab* **14**, 151–153.
- Höckel M & Vaupel P (2001) Tumor hypoxia: definitions and current clinical, biologic, and molecular aspects. *J Natl Cancer Inst* **93**, 266–276.
- Guillaumond F, Leca J, Olivares O, Lavaut MN, Vidal N, Berthezène P, Dusetti N, Loncle C, Calvo E, Turrini O *et al.* (2013) Strengthened glycolysis under hypoxia supports tumor symbiosis and hexosamine biosynthesis in pancreatic adenocarcinoma. *Proc Natl Acad Sci U S A* **110**, 3919–3924.
- Yun J, Rago C, Cheong I, Pagliarini R, Angenendt P, Rajagopalan H, Schmidt K, Willson J, Markowitz S, Zhou S *et al.* (2009) Glucose deprivation contributes to the development of KRAS pathway mutations in tumor cells. *Science* **325**, 1555–1559.
- Graeber T, Osmanian C, Jacks T, Housman D, Koch C, Lowe S & Giaccia A (1996) Hypoxia-mediated selection of cells with diminished apoptotic potential in solid tumours. *Nature* **379**, 88–91.
- Vander Heiden MG, Lunt SY, Dayton TL, Fiske BP, Israelsen WJ, Mattaini KR, Vokes NI, Stephanopoulos G, Cantley LC, Metallo CM *et al.* (2012) Metabolic pathway alterations that support cell proliferation. *Cold Spring Harb Symp Quant Biol* **76**, 325–334.
- Vander Heiden M (2011) Targeting cancer metabolism: a therapeutic window opens. *Nat Rev Drug Discov* **10**, 671–684.
- Koppenol W, Bounds P & Dang C (2011) Otto Warburg's contributions to current concepts of cancer metabolism. *Nat Rev Cancer* **11**, 325–337.
- Vander Heiden MG, Cantley LC & Thompson CB (2009) Understanding the Warburg effect: the metabolic requirements of cell proliferation. *Science* **324**, 1029–1033.
- Warburg O (1956) On the origin of cancer cells. *Science* **123**, 309–314.
- Bouché C, Serdy S, Kahn C & Goldfine A (2004) The cellular fate of glucose and its relevance in type 2 diabetes. *Endocr Rev* **25**, 807–830.
- Buse M (2006) Hexosamines, insulin resistance, and the complications of diabetes: current status. *Am J Physiol Endocrinol Metab* **290**, E1–E8.
- Wells L, Vosseller K & Hart GW (2003) A role for N-acetylglucosamine as a nutrient sensor and mediator of insulin resistance. *Cell Mol Life Sci* **60**, 222–228.

- 21 Dennis J, Nabi I & Demetriou M (2009) Metabolism, cell surface organization, and disease. *Cell* **139**, 1229–1241.
- 22 Dennis J, Lau K, Demetriou M & Nabi I (2009) Adaptive regulation at the cell surface by N-glycosylation. *Traffic* **10**, 1569–1578.
- 23 Wellen K, Lu C, Mancuso A, Lemons J, Ryzcko M, Dennis J, Rabinowitz J, Collier H & Thompson C (2010) The hexosamine biosynthetic pathway couples growth factor-induced glutamine uptake to glucose metabolism. *Genes Dev* **24**, 2784–2799.
- 24 Slawson C & Hart GW (2011) O-GlcNAc signalling: implications for cancer cell biology. *Nat Rev Cancer* **11**, 678–684.
- 25 Ying H, Kimmelman A, Lyssiotis C, Hua S, Chu G, Fletcher-Sananikone E, Locasale J, Son J, Zhang H, Coloff J *et al.* (2012) Oncogenic Kras maintains pancreatic tumors through regulation of anabolic glucose metabolism. *Cell* **149**, 656–670.
- 26 Ma Z, Vocadlo D & Vosseller K (2013) Hyper-O-GlcNAcylation is anti-apoptotic and maintains constitutive NF- κ B activity in pancreatic cancer cells. *J Biol Chem* **288**, 15121–15130.
- 27 Caldwell S, Jackson S, Shahriari K, Lynch T, Sethi G, Walker S, Vosseller K & Reginato M (2010) Nutrient sensor O-GlcNAc transferase regulates breast cancer tumorigenesis through targeting of the oncogenic transcription factor FoxM1. *Oncogene* **29**, 2831–2842.
- 28 Siddle K (2012) Molecular basis of signaling specificity of insulin and IGF receptors: neglected corners and recent advances. *Front Endocrinol* **3**, 34.
- 29 Siddle K (2011) Signalling by insulin and IGF receptors: supporting acts and new players. *J Mol Endocrinol* **47**, 10.
- 30 Kalaany N & Sabatini D (2009) Tumours with PI3K activation are resistant to dietary restriction. *Nature* **458**, 725–731.
- 31 Keller SR, Lamphere L, Lavan BE, Kuhne MR & Lienhard GE (1993) Insulin and IGF-I signaling through the insulin receptor substrate 1. *Mol Reprod Dev* **35**, 346–351. discussion 351–352.
- 32 Lavan B & Lienhard G (1993) The insulin-elicited 60-kDa phosphotyrosine protein in rat adipocytes is associated with phosphatidylinositol 3-kinase. *J Biol Chem* **268**, 5921–5928.
- 33 Myers M, Backer J, Sun X, Shoelson S, Hu P, Schlessinger J, Yoakim M, Schaffhausen B & White M (1992) IRS-1 activates phosphatidylinositol 3'-kinase by associating with src homology 2 domains of p85. *Proc Natl Acad Sci U S A* **89**, 10350–10354.
- 34 Jones D, Foulger R, Keune WJ, Bultsma Y & Divecha N (2013) PtdIns5P is an oxidative stress-induced second messenger that regulates PKB activation. *FASEB J* **27**, 1644–1656.
- 35 Sarbassov D, Guertin D, Ali S & Sabatini D (2005) Phosphorylation and regulation of Akt/PKB by the rictor-mTOR complex. *Science* **307**, 1098–1101.
- 36 Park J, Feng J, Li Y, Hammarsten O, Brazil D & Hemmings B (2009) DNA-dependent protein kinase-mediated phosphorylation of protein kinase B requires a specific recognition sequence in the C-terminal hydrophobic motif. *J Biol Chem* **284**, 6169–6174.
- 37 Feng J, Park J, Cron P, Hess D & Hemmings B (2004) Identification of a PKB/Akt hydrophobic motif Ser-473 kinase as DNA-dependent protein kinase. *J Biol Chem* **279**, 41189–41196.
- 38 Cohen P, Alessi DR & Cross DA (1997) PDK1, one of the missing links in insulin signal transduction? *FEBS Lett* **410**, 3–10.
- 39 Kang J, Park S, Ji S, Jang I, Park S, Kim H, Kim SM, Yook J, Park YI, Roth JA *et al.* (2009) O-GlcNAc protein modification in cancer cells increases in response to glucose deprivation through glycogen degradation. *J Biol Chem* **284**, 34777–34784.
- 40 Schnier J, Nishi K, Monks A, Gorin F & Bradbury E (2003) Inhibition of glycogen phosphorylase (GP) by CP-91,149 induces growth inhibition correlating with brain GP expression. *Biochem Biophys Res Commun* **309**, 126–134.
- 41 Taylor R, Geisler T, Chambers J & McClain D (2009) Up-regulation of O-GlcNAc transferase with glucose deprivation in HepG2 cells is mediated by decreased hexosamine pathway flux. *J Biol Chem* **284**, 3425–3432.
- 42 Taylor R, Parker G, Hazel M, Soesanto Y, Fuller W, Yazzie M & McClain D (2008) Glucose deprivation stimulates O-GlcNAc modification of proteins through up-regulation of O-linked N-acetylglucosaminyltransferase. *J Biol Chem* **283**, 6050–6057.
- 43 Whelan SA, Dias WB, Thiruneelakantapillai L, Lane MD & Hart GW (2010) Regulation of insulin receptor substrate 1 (IRS-1)/AKT kinase-mediated insulin signaling by O-Linked beta-N-acetylglucosamine in 3T3-L1 adipocytes. *J Biol Chem* **285**, 5204–5211.
- 44 Vosseller K, Wells L, Lane MD & Hart GW (2002) Elevated nucleocytoplasmic glycosylation by O-GlcNAc results in insulin resistance associated with defects in Akt activation in 3T3-L1 adipocytes. *Proc Natl Acad Sci U S A* **99**, 5313–5318.
- 45 Park S, Ryu J & Lee W (2005) O-GlcNAc modification on IRS-1 and Akt2 by PUGNAc inhibits their phosphorylation and induces insulin resistance in rat primary adipocytes. *Exp Mol Med* **37**, 220–229.
- 46 Arias E, Kim J & Cartee G (2004) Prolonged incubation in PUGNAc results in increased protein O-linked glycosylation and insulin resistance in rat skeletal muscle. *Diabetes* **53**, 921–930.
- 47 Robinson K, Ball L & Buse M (2007) Reduction of O-GlcNAc protein modification does not prevent insulin

- resistance in 3T3-L1 adipocytes. *Am J Physiol Endocrinol Metab* **292**, 90.
- 48 Macauley M, Bubb A, Martinez-Fleites C, Davies G & Vocadlo D (2008) Elevation of global O-GlcNAc levels in 3T3-L1 adipocytes by selective inhibition of O-GlcNAcase does not induce insulin resistance. *J Biol Chem* **283**, 34687–34695.
- 49 Macauley M, He Y, Gloster T, Stubbs K, Davies G & Vocadlo D (2010) Inhibition of O-GlcNAcase using a potent and cell-permeable inhibitor does not induce insulin resistance in 3T3-L1 adipocytes. *Chem Biol* **17**, 937–948.
- 50 Hanover J, Forsythe M, Hennessey P, Brodigan T, Love D, Ashwell G & Krause M (2005) A *Caenorhabditis elegans* model of insulin resistance: altered macronutrient storage and dauer formation in an OGT-1 knockout. *Proc Natl Acad Sci U S A* **102**, 11266–11271.
- 51 Love D, Ghosh S, Mondoux M, Fukushige T, Wang P, Wilson M, Iser W, Wolkow C, Krause M & Hanover J (2010) Dynamic O-GlcNAc cycling at promoters of *Caenorhabditis elegans* genes regulating longevity, stress, and immunity. *Proc Natl Acad Sci U S A* **107**, 7413–7418.
- 52 Park S, Park SH, Baek J, Jy Y, Kim K, Roth J \ddot{A} , Cho J & Choe KM (2011) Protein O-GlcNAcylation regulates *Drosophila* growth through the insulin signaling pathway. *Cell Mol Life Sci* **68**, 3377–3384.
- 53 Klein A, Berkaw M, Buse M & Ball L (2009) O-linked N-acetylglucosamine modification of insulin receptor substrate-1 occurs in close proximity to multiple SH2 domain binding motifs. *Mol Cell Proteomics* **8**, 2733–2745.
- 54 Ball L, Berkaw M & Buse M (2006) Identification of the major site of O-linked beta-N-acetylglucosamine modification in the C terminus of insulin receptor substrate-1. *Mol Cell Proteomics* **5**, 313–323.
- 55 Krzeslak A, Józwiak P & Lipinska A (2011) Down-regulation of β -N-acetyl-D-glucosaminidase increases Akt1 activity in thyroid anaplastic cancer cells. *Oncol Rep* **26**, 743–749.
- 56 Morrish F, Isern N, Sadilek M, Jeffrey M & Hockenbery D (2009) c-Myc activates multiple metabolic networks to generate substrates for cell-cycle entry. *Oncogene* **28**, 2485–2491.
- 57 Isakoff SJ, Engelman JA, Irie HY, Luo J, Brachmann SM, Pearlman RV, Cantley LC & Brugge JS (2005) Breast cancer-associated PIK3CA mutations are oncogenic in mammary epithelial cells. *Cancer Res* **65**, 10992–11000.
- 58 Pelletier J, Bellot Gg, Gounon P, Lacas-Gervais S, Pouyssegur J & Mazure N (2012) Glycogen synthesis is induced in hypoxia by the hypoxia-inducible factor and promotes cancer cell survival. *Front Oncol* **2**, 18.
- 59 Lee W-NP, Guo P, Lim S, Bassilian S, Lee S, Boren J, Cascante M, Go V & Boros L (2004) Metabolic sensitivity of pancreatic tumour cell apoptosis to glycogen phosphorylase inhibitor treatment. *Br J Cancer* **91**, 2094–2100.
- 60 Favaro E, Bensaad K, Chong M, Tennant D, Ferguson D, Snell C, Steers G, Turley H, Li JL, Günther UL *et al.* (2012) Glucose utilization via glycogen phosphorylase sustains proliferation and prevents premature senescence in cancer cells. *Cell Metab* **16**, 751–764.
- 61 Clark J, Anderson KE, Juvin V, Smith TS, Karpe F, Wakelam MJ, Stephens LR & Hawkins PT (2011) Quantification of PtdInsP3 molecular species in cells and tissues by mass spectrometry. *Nat Methods* **8**, 267–272.